

NMR studies of overdoped $Y_{1-x}Ca_xBa_2Cu_3O_{7-\delta}$

G. V. M. Williams and J. L. Tallon

The New Zealand Institute for Industrial Research and Development, P.O. Box 31310, Lower Hutt, New Zealand

R. Michalak and R. Dupree

Department of Physics, University of Warwick, Coventry CV4 7AL, United Kingdom

(Received 30 July 1997; revised manuscript received 20 November 1997)

^{89}Y NMR and ^{17}O NMR data from overdoped $Y_{1-x}Ca_xBa_2Cu_3O_{7-\delta}$ superconductors is presented and interpreted in terms of a peak in the density of states (DOS) that is pinned to the Fermi level and grows with progressive overdoping. This is in contrast to the underdoped side where there occurs a gap in the DOS pinned to the Fermi level. The data, which may be common to the high-temperature superconducting cuprates, are inconsistent with previously proposed models of phase separation or an increasing density of local moments. [S0163-1829(98)03310-4]

INTRODUCTION

There exist a variety of theories for the origin of superconductivity in the high-temperature superconducting cuprates but it is our opinion that none explain all of the experimental data. Of particular importance is the superconducting phase diagram. It has already been shown that a normal-state pseudogap with a d -wave-like symmetry exists above T_c for hole concentrations p less than 0.19 (Refs. 1–3) and there also exists a universal dependence of T_c on hole concentration, approximated by $T_c/T_{c,Max} = 1 - 82.6(p - 0.16)^2$.⁴ Loram *et al.* have shown that, for underdoped superconductors, the normal-state pseudogap removes spectral weight and hence leads to a decrease in T_c even though the spectral gap is constant or even increasing in the underdoped region.⁵ The overdoped superconductors with $p \geq 0.19$ do not display a normal-state pseudogap but, as in the underdoped region, there is a rapid decrease in magnitude of the superconducting order parameter⁶ and in λ_{ab}^{-2} ,⁷ where λ_{ab} is the in-plane penetration depth. It has previously been shown that the van-Hove singularity (vHs), postulated to reside at optimal doping in order to explain maximal T_c at $p = 0.16$, is not apparent in either the NMR, heat capacity, or susceptibility data,⁸ nonetheless the NMR shift for fully oxygenated $YBa_2Cu_3O_{7-\delta}$ displays a small Curie-like temperature dependence that we will show grows with further overdoping.⁹

In this paper we report ^{17}O NMR and ^{89}Y magic angle spinning (MAS) NMR measurements on overdoped $Y_{1-x}Ca_xBa_2Cu_3O_{7-\delta}$. Unlike previous studies we use the same $Y_{1-x}Ca_xBa_2Cu_3O_{7-\delta}$ superconductor for each oxygen concentration and hence eliminate sample-dependent effects due to Ca disorder. The advantage of the $Y_{1-x}Ca_xBa_2Cu_3O_{7-\delta}$ superconductor is that we have been able to produce good quality samples in which Ca resides almost wholly on the Y site and, in conjunction with a post-processing technique, increase the hole concentration deep into the overdoped region resulting in T_c values as low as 47 K. Another advantage is that we are able to use ^{89}Y to probe the local spin susceptibility and bonding environment. Un-

like ^{17}O NMR, ^{65}Cu NMR and susceptibility measurements, ^{89}Y NMR does not suffer from quadrupole broadening due to local electric-field gradient or paramagnetic impurity effects. ^{17}O and ^{65}Cu NMR measurements also need to be performed on aligned samples and the experimental uncertainty in determining the peak position can hide small temperature-dependent changes in the peak position. We show that the data is consistent with a peak in the density of states (DOS) which grows with overdoping in contrast to the underdoped data where there is a gap in the DOS. In both cases these features are pinned to the Fermi level.

EXPERIMENTAL DETAILS

$Y_{1-x}Ca_xBa_2Cu_3O_{7-\delta}$ samples were synthesized by initially decomposing a stoichiometric mixture of Y_2O_3 , $Ca(NO_3)_2$, $Ba(NO_3)_2$ and CuO in air at 700 °C for 1 h. This was followed by reactions in air at 900 °C for 6 h and 915 °C, 930 °C, 940 °C, and 950 °C for 24 h. The samples were then heated at 980 °C in O_2 at 1 bar for 6 h followed by rapid cooling to 350 °C and then 350 °C for 48 h to achieve maximum overdoping. The samples were reground after each sinter. The hole concentrations were varied by annealing in nitrogen/oxygen gas mixtures at a variety of oxygen partial pressures and temperatures. X-ray-diffraction (XRD) analysis showed that the samples were single phase and there was no evidence of the $Ba_4CaCu_3O_8$ and $BaCuO_2$ impurity phases that are known to occur when there is partial Ca substitution of Ba. Samples were ^{17}O exchanged by annealing in 10% ^{17}O enriched O_2 and at a variety of temperatures in order to control their oxygen stoichiometry and hence their hole concentrations. The ^{17}O exchanged samples were c -axis aligned in a magnetic field of 11.74 T and the alignment was checked using XRD. ac susceptibility measurements were used to determine the T_c values. The hole concentration p was determined from thermoelectric power¹⁰ and from the relation $T_c/T_{c,Max} = 1 - 82.6(p - 0.16)^2$.⁴

Variable temperature ^{89}Y NMR measurements were performed at temperatures of 110 to 350 K using a Varian Unity 500 spectrometer and a 11.74 T superconducting magnet.

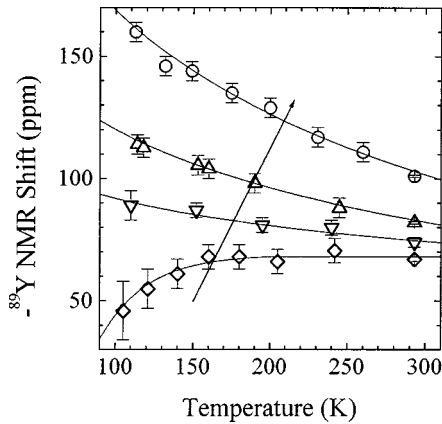


FIG. 1. Plot of the ^{89}Y NMR shift against temperature for an overdoped $Y_{0.8}\text{Ca}_{0.2}\text{Ba}_2\text{Cu}_3\text{O}_{7-\delta}$ superconductor with T_c and p values of 47.5 K, $p=0.234$ (\circ), 72.1 K, $p=0.206$ (Δ), 80.1 K, $p=0.192$ (∇), and 86 K, $p=0.173$ (\diamond). The solid line are fits to the data using the density of states in Fig. 5 and the solid line indicates increasing hole concentration.

Magic angle spinning at a frequency >2.5 kHz was used to remove dipole-dipole coupling and hence reduce the spectral linewidth. The spectra were collected using the $90^\circ\text{-}\tau\text{-}180^\circ$ spin-echo technique where τ was set to one rotor period. The NMR shifts were referenced to a 1M aqueous solution of YCl_3 . ^{17}O NMR measurements were made from 10 to 300 K using a Bruker MSL 360 spectrometer and a 8.45 T superconducting magnet. The $90^\circ\text{-}\tau\text{-}180^\circ$ spin-echo technique was used to collect the data and the NMR shifts were referenced to H_2O .

RESULTS AND ANALYSIS

We present in Fig. 1 the temperature-dependent ^{89}Y MAS NMR shifts from the overdoped $Y_{0.8}\text{Ca}_{0.2}\text{Ba}_2\text{Cu}_3\text{O}_{7-\delta}$ sample for a variety of hole concentrations. The direction of increasing p is shown by the arrow. Leaving aside the slightly overdoped sample for which the pseudogap is still present, it can be seen that the ^{89}Y MAS NMR shifts display a Curie-like temperature dependence that becomes more pronounced as the hole concentration is increased. This Curie-like temperature dependence is also observed in overdoped $Y_{0.9}\text{Ca}_{0.1}\text{Ba}_2\text{Cu}_3\text{O}_{7-\delta}$ and $\text{YBa}_2\text{Cu}_3\text{O}_{7-\delta}$ (Refs. 9 and 11) ^{89}Y MAS NMR data as can be seen in Fig. 2. The upturn in the $Y_{1-x}\text{Ca}_x\text{Ba}_2\text{Cu}_3\text{O}_{7-\delta}$ ^{89}Y MAS NMR shift is also mirrored in the temperature dependence of the ^{17}O NMR data. This is shown in Fig. 3 where we plot the ^{17}O NMR shift of the central ^{17}O NMR peak and the ^{17}O NMR shift of the first ^{17}O satellite for an overdoped $Y_{0.8}\text{Ca}_{0.2}\text{Ba}_2\text{Cu}_3\text{O}_{7-\delta}$ sample with $T_c=55$ K where the magnetic field is along the c axis. For comparison we also show the ^{89}Y MAS NMR shift (open triangles). It is clear that the increase in the NMR shift with decreasing temperature exists in both the ^{17}O and ^{89}Y NMR spectra and reflects the temperature dependence of the spin susceptibility. This is consistent with previous studies^{12,13} that showed that the NMR shift could be expressed as $K=\sum_j A_j \chi_s/g\mu_B + \sigma$ where A_j is the transferred hyperfine coupling constant (negative for ^{89}Y), χ_s is the static spin susceptibility, g is the electron g factor, μ_B is the Bohr magneton, and σ is the

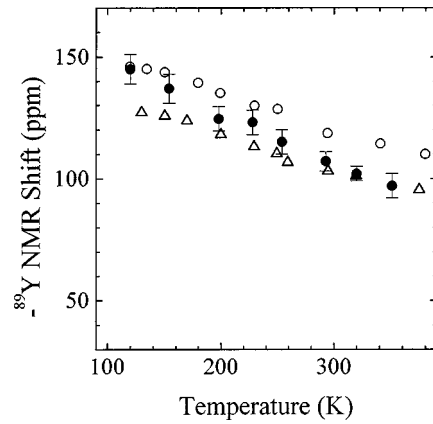


FIG. 2. Plot of the ^{89}Y NMR shift against temperature for overdoped $\text{YBa}_2\text{Cu}_3\text{O}_{7-\delta}$ (\circ) (Ref. 9), $\text{YBa}_2\text{Cu}_3\text{O}_{7-\delta}$ (Δ) (Ref. 11), and $Y_{0.9}\text{Ca}_{0.1}\text{Ba}_2\text{Cu}_3\text{O}_{7-\delta}$ ($T_c=68$ K) (\bullet) samples.

temperature-independent chemical shift. The Curie-like ^{89}Y MAS NMR shift is not unique to the overdoped $Y_{1-x}\text{Ca}_x\text{Ba}_2\text{Cu}_3\text{O}_{7-\delta}$ superconductor with double CuO_2 planes. It has also been observed in overdoped $\text{TlSr}_2(\text{Lu}_{1-x}\text{Ca}_x)\text{Cu}_2\text{O}_y$ (susceptibility measurements¹⁴), $\text{Tl}_2\text{Ba}_2\text{CuO}_{6+\delta}$ (susceptibility measurements¹⁵), $\text{Bi}_2\text{Sr}_2\text{Ca}_{n-1}\text{Cu}_n\text{O}_{2n+4}$ [^{17}O NMR (Ref. 16)] and is particularly strong in $\text{La}_{2-x}\text{Sr}_x\text{CuO}_4$ (^{17}O NMR,¹⁷ susceptibility¹⁸ and heat capacity¹⁹ measurements). We emphasize that, while bulk susceptibility measurements may be influenced by paramagnetic impurities, the effects probed by the NMR shifts are intrinsic.

Previously, it was found from ^{89}Y NMR studies on $Y_{1-x}\text{Ca}_x\text{Ba}_2\text{Cu}_3\text{O}_{7-\delta}$ samples, which were not as overdoped as the samples in the present study, that there appeared to exist a universal curve, $^{89}\Lambda(T)=^{89}\Gamma(T)/[^{89}\text{K}(T)-^{89}\sigma]$ where $^{89}\Gamma(T)$ is the ^{89}Y MAS NMR linewidth.¹¹ In the previous study the Ca content in the overdoped samples, rather than δ , was varied. It was concluded that the universal curve originates from a temperature-dependent antiferromagnetic

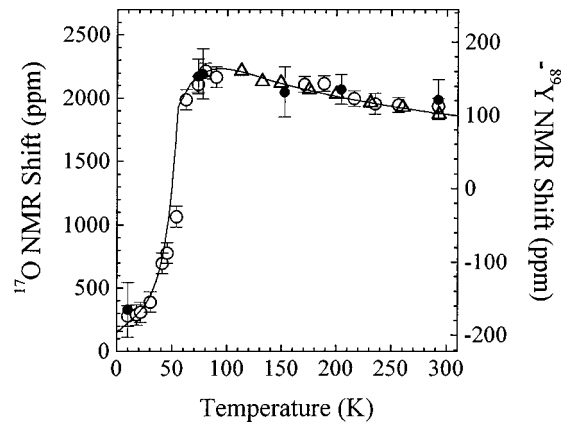


FIG. 3. Plot of the temperature dependence of the ^{17}O NMR shift for the central line (\circ) and the first satellite (\bullet) from an overdoped $Y_{0.8}\text{Ca}_{0.2}\text{Ba}_2\text{Cu}_3\text{O}_{7-\delta}$ sample with $T_c=55$ K where the magnetic field is parallel to the c axis. Also shown is the ^{89}Y NMR shift from a slightly more overdoped $Y_{0.8}\text{Ca}_{0.2}\text{Ba}_2\text{Cu}_3\text{O}_{7-\delta}$ sample with $T_c=47.5$ K (Δ). The solid curve is the model in the text with $E_g(0)/k_B=130$ K, $\Delta(0)/k_B=200$ K, and the initial density of states in Fig. 5 with $y=0.87$.

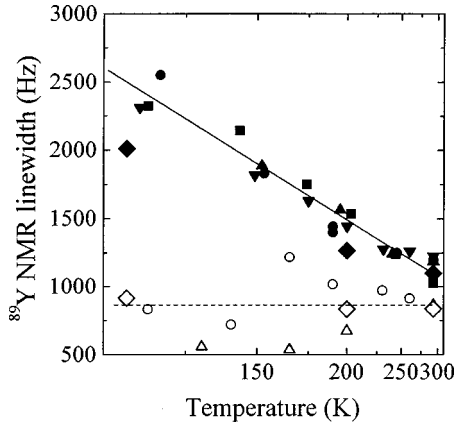


FIG. 4. Plot of the ^{89}Y MAS NMR linewidth against inverse temperature for $\text{Y}_{0.8}\text{Ca}_{0.2}\text{Ba}_2\text{Cu}_3\text{O}_{7-\delta}$ samples with $T_c = 47.5$ K, $p = 0.234$ (∇), $T_c = 72.1$ K, $p = 0.206$ (\bullet), $T_c = 80.1$ K, $p = 0.192$ (\blacktriangle), $T_c = 83.2$ K, $p = 0.136$ (\blacksquare), $T_c = 65.8$ K, $p = 0.105$ (\circ), and $T_c = 47.5$ K, $p = 0.086$ (\triangle). The solid and dashed lines are guides to the eye. Also included is the ^{89}Y MAS NMR linewidths expected if there is Ca induced disorder with $s_p = 0.014$ and $s_\sigma = 360$ Hz for $p \geq 0.136$ (\blacklozenge) and $s_p = 0.0018$ and $s_\sigma = 290$ Hz for $p \leq 0.105$ (\diamond).

correlation length $\xi_c(T)$ that is independent of hole concentration for overdoped superconducting cuprates. It is apparent from Fig. 4 that this is not the case. Here we plot $^{89}\Gamma(T)$ against $1/T$. It can be seen that $^{89}\Gamma(T)$ has a Curie-like temperature dependence, independent of hole concentration for $p \geq 0.136$. This Curie-like temperature dependence is also seen in $^{17}\Gamma(T)$. Thus, in conjunction with Fig. 1, it is evident that a universal function $^{89}A(T) = ^{89}\Gamma(T) / [^{89}\text{K}(T) - ^{89}\sigma]$ does not exist. We attribute the original correlation to the varying Ca concentrations used in the study because although the Curie-like temperature dependence in $^{89}\Gamma(T)$ is independent of p for each Ca concentration the $1/T$ coefficient increases with increasing Ca concentration for $p \geq 0.136$. This is a disorder effect²⁰ that fortuitously roughly offsets the increasing $1/T$ coefficient in $^{89}\text{K}(T) - ^{89}\sigma$ that is a doping effect. When the Ca content is fixed, only the doping state may be altered and $^{89}\Lambda(T)$ varies accordingly.

The Curie-like temperature dependence of ^{89}K , ^{17}K , $^{89}\Gamma$, and $^{17}\Gamma$ cannot be attributed to magnetic impurities or the formation of local moments as suggested elsewhere.^{21,22} Previous NMR and susceptibility studies on $\text{YBa}_2\text{Cu}_3\text{O}_{7-\delta}$ and $\text{YBa}_2\text{Cu}_4\text{O}_8$ with Zn and Ni impurities were interpreted in terms of a local moment near the impurity leading to a spin-density oscillation and hence a broadening of the NMR peak and, in the case of Zn substitution, a satellite peak with a Curie-like temperature dependence.^{23–26} In this model $\Gamma = a_0x/T$ and $\text{K} = a_1x/T + a_2 + \sigma$ where x is the concentration of magnetic impurities or local moments. It is clear that K would seem to follow this type of temperature and hole concentration-dependence but Γ , while being Curie-like for $p \geq 0.136$, is independent of hole concentration. Neither can the data in Figs. 1, 2, 3, and 4 be explained by nanoscale or macroscopic phase separation.²⁷ In the phase separation model it is assumed that a vHS exists at optimal doping ($p = 0.16$). For the underdoped superconductors it has been suggested that the low hole concentration can lead to ‘‘hole bunching’’ and hence nanoscale phase separation into the metallic $p = 0.16$ phase and insulating antiferromagnetic p

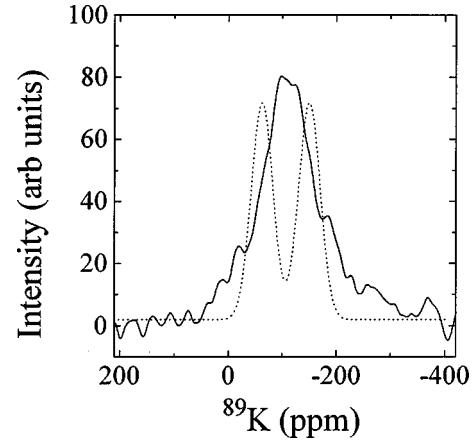


FIG. 5. Plot of the ^{89}Y MAS NMR spectra at 150 K from a $\text{Y}_{0.8}\text{Ca}_{0.2}\text{Ba}_2\text{Cu}_3\text{O}_{7-\delta}$ sample with $p = 0.2059$. Also shown is the anticipated phase separation spectra (dotted curve).

$= 0$ phase, the net result being a ‘‘phase-separated charge-density wave.’’ However, it has been shown that NMR and thermodynamic data for $p \leq 0.16$ cannot be modelled by a vHS, either in a phase separation model or with the Fermi level sweeping through a vHS.¹ If nanoscale phase separation occurred in the overdoped region with the other phase being $p \sim 0.27$ then the Curie-like $1/T$ coefficient in both $\text{K}(T)$ and $\Gamma(T)$ will initially increase as the hole concentration is increased, provided the NMR spectra from each phase is sufficiently broad. However this is not the case in our samples where $^{89}\Gamma(300 \text{ K}) \approx 1.2 \text{ kHz}$ and hence the ^{89}Y MAS NMR spectra at low temperatures is expected to display two peaks. It is apparent in Fig. 5 that the low-temperature spectra display only one peak. Here we plot the ^{89}Y NMR MAS spectra at 150 K and $p = 0.2059$ (solid curve). Although it is not possible to measure the anticipated $p = 0.27$ phase in the $\text{Y}_{1-x}\text{Ca}_x\text{Ba}_2\text{Cu}_3\text{O}_{7-\delta}$ superconductor we can obtain an underestimate for the expected phase separated phase using the $p = 0.1729$ and $p = 0.2344$ ^{89}Y MAS NMR data. The result is shown in Fig. 5 where we use $\Gamma(150 \text{ K}) = \Gamma(300 \text{ K})$. It is clear that a phase separation model cannot describe the data. Consequently, even though phase separation has been suggested from early neutron-diffraction experiments on $\text{La}_{2-x}\text{Sr}_x\text{CuO}_4$,²⁸ it is inconsistent with the present data. More recent neutron-diffraction studies on $\text{La}_{2-x}\text{Sr}_x\text{CuO}_4$ indicate that, with appropriate preparation, these samples are homogeneous.²⁹

As mentioned above, models based on a vHS where the Fermi level sweeps through the vHS at $p = 0.16$ are unable to explain the NMR, heat capacity, and susceptibility measurements for all hole concentrations. Likewise models of the double CuO_2 layer compounds based upon an exchange splitting of the bands cannot describe the data.³⁰ These models predict an NMR shift that does not converge to the chemical shift at $T = 0$ with progressive underdoping and are inconsistent with a recent study which showed that intraplanar impurities (e.g., Zn and Ni) have a dramatic effect on T_c while interplanar impurities (e.g., Ca exchanged for Y between the CuO_2 planes) result in a negligible change in T_c .²⁰ It was shown that the susceptibility, NMR and thermopower data are entirely consistent with only weak exchange coupling between the CuO_2 planes.

We propose a simple model to explain the NMR shift in the overdoped samples in terms of a peak in the DOS that grows for hole concentrations $p \geq 0.17$. We model the data in Fig. 1 using the Pauli spin susceptibility

$$\chi_s = \mu_B^2 \int_{-\infty}^{\infty} N(E) [-\partial f(E)/\partial E] dE, \quad (1)$$

where $N(E)$ is the density of states and $f(E)$ is the Fermi function. It is apparent from Eq. (1) that an energy-dependent DOS with a peak pinned to the Fermi level will lead to a Knight shift that increases with decreasing temperature. Evidence for a peak in the DOS at the Fermi level has already been provided by heat capacity and susceptibility measurements on overdoped $La_{2-x}Sr_xCuO_4$.¹⁹ Consequently, we model the ^{89}Y NMR data with a two-dimensional energy-dependent DOS,

$$N(E) = (1-y)N_{Fg} + yN_{vHS}(E), \quad (2)$$

where N_{Fg} is the energy-independent DOS, $N_{vHS}(E)$ is the energy-dependent DOS and y is the ‘‘amplitude’’ of the energy-dependent peak in the DOS. For the energy-independent DOS we use the energy dispersion, $E(\mathbf{k}) = \hbar^2 k^2/2m^*$, while for the energy-dependent DOS we use a nearest-neighbor hopping dispersion, $E(\mathbf{k}) = -2t[\cos(k_x a) + \cos(k_y a)]$, where t is related to the nearest-neighbor hopping probability. The motivation for using Eq. (2) to model the DOS is that for the underdoped superconductors the $E(\mathbf{k}) = \hbar^2 k^2/2m^*$ energy dispersion with a normal-state pseudogap existing for $p \leq 0.19$ has proven successful in modeling the heat capacity, susceptibility and NMR Knight-shift data.^{1,2,5} For the overdoped superconductors the nearest-neighbor hopping dispersion conveniently provides a peak in the DOS and the appearance of a vHS peak near $p = 0.27$ with the Fermi level sweeping below the peak energy for $p > 0.27$, consistent with the observed change in the Hall coefficient and the maximum in the susceptibility and entropy data for $La_{2-x}Sr_xCuO_4$.^{19,31} As shown previously, the effect of the normal-state pseudogap in the samples with $p < 0.19$ can be accounted for with an energy dispersion $E(\mathbf{k}) = [\epsilon(\mathbf{k})^2 + \Delta(\mathbf{k})^2]^{1/2}$ where $\epsilon(\mathbf{k}) = \hbar^2 k^2/2m^*$ and $\Delta(\mathbf{k}) = E_g(\mathbf{k})$ for temperatures above T_c . $E_g(\mathbf{k}) = E_g |\cos(2\theta)|$ is the anisotropic pseudogap energy,^{2,6} but we stress that there is no order parameter above T_c . Below T_c , $\Delta(\mathbf{k}) = [\Delta'(\mathbf{k})^2 + E_g(\mathbf{k})^2]^{1/2}$ where $\Delta'(\mathbf{k})$ is the superconducting order parameter with d -wave symmetry.

We note that there are at least four other models that attempt to describe the thermodynamic, susceptibility and NMR data above T_c . In one model the temperature-dependence of the NMR data is attributed to exchange coupling for superconductors with two CuO_2 planes per unit cell and a spin-density-wave instability for superconductors with only one CuO_2 plane per unit cell.^{30,32} In another model the normal-state pseudogap is attributed to precursor pairing without long-range phase coherence and superconductivity occurring when long-range phase coherence is established.³³ In the nearly antiferromagnetic Fermi liquid (NAFL) model the NMR data is described by scaling regimes: mean-field for $T > T_{cr}$, pseudoscaling for $T^* < T < T_{cr}$ and a pseudogap of magnetic origin for $T < T^*$.³⁴⁻³⁶ Within the NAFL model there is an abrupt transition at T^* to a pseudogap where the

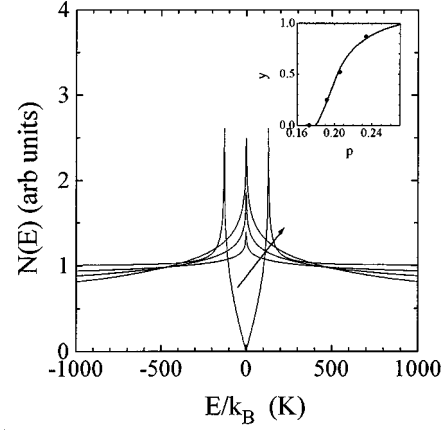


FIG. 6. Plot of the density of states, $N(E)$, used to model the data in Figs. 1 and 3. The arrow indicates the direction of increasing hole concentration. The values of y are plotted in the insert. The solid curve is a guide to the eye.

pseudogap energy E_g is temperature independent below T^* .³⁵ In the NAFL model the ^{89}Y NMR shift data for $p = 0.1729$ would have $T_{cr} \sim 150$ K. In the model of Eremin *et al.*³⁷ the NMR data above T_c is explained by the appearance of a pseudogap at T^* originating from a charge-density-wave instability. We show elsewhere that the charge-density-wave model is negated by the absence of an isotope effect in the pseudogap³⁸ and that models with a normal-state pseudogap more or less abruptly appearing at a temperature T^* are inconsistent with the thermodynamic, susceptibility, and NMR Knight-shift data.³⁹

The interpretation of the $p \leq 0.19$ data in terms of the NAFL model with T_{cr} increasing with decreasing p or a pseudogap with E_g increasing with decreasing p is of secondary concern in this paper. Here we are specifically interested in the region $p \geq 0.19$. We show in Fig. 1 (solid curves) that the DOS in Eq. (2) provides an excellent fit to the data. The resultant DOS used to fit the data is shown in Fig. 6. The data for $p = 0.1729$ is modeled with a nonzero normal-state gap to account for the decrease in the NMR shift for temperatures less than 160 K. The insert to Fig. 6 shows the p dependence of y in Eq. (2) where it can be seen that it appears to progress to 1 when $p = 0.27$, i.e., at the superconductor/metal transition where $T_c = 0$.

While a growing peak in the DOS provides an excellent fit to the NMR shift data it does not immediately lead to an explanation for the Curie-like and p -independent linewidth data in Fig. 4 when $p \geq 0.136$. One possibility is disorder effects induced by Ca substitution as found by a previous study of the $Y_{1-x}Ca_xBa_{2-x}La_xCu_4O_8$, $YBa_2Cu_{4-z}Zn_zO_8$, and $YBa_2Cu_{4-z}Ni_zO_8$ superconductors.²⁰ We show in Fig. 4 the expected $^{89}Y\Gamma(T)$ if there existed random hole concentration and chemical shift disorder with $s_p = 0.014$ and $s_\sigma = 360$ Hz for $p \geq 0.136$ (closed large diamonds) where s_p and s_σ are the standard deviations in the hole concentration and chemical shift. For $p \leq 0.105$ we use $s_p = 0.0018$ and $s_\sigma = 290$ Hz (large open diamonds). It can be seen that this explanation does result in a Curie-like $^{89}Y\Gamma(T)$ for $p \geq 0.136$ and a temperature-independent Γ for $p \leq 0.105$. The origin of such a narrowing in the distribution of p is uncertain but

could be associated with the incipient phase separation that seems to occur for $p \leq 0.105$.⁴⁰

We show in Fig. 3 (solid curve) that the decrease in the ^{17}O NMR shift below 85 K but above $T_c = 55$ K could be interpreted in terms of a normal-state pseudogap. Here, to illustrate, we assume the pseudogap to have d -wave-like symmetry with a pseudogap energy E_g that is temperature dependent, decreasing from $E_g = 130k_B$ at $T=0$ to $E_g = 0$ at $T^* = E_g$. However both angle-resolved photoemission spectroscopy (ARPES Ref. 41) and heat capacity data⁶ have shown that the pseudogap is absent for this hole concentration. Rather in some cases the heat capacity shows a split transition with a small mean-field step at about 84 K.⁴² This would result in a downturn in $K(T)$ as shown in Fig. 3 where $<12\%$ of the sample does not have fully oxygen loaded chains.

It is important to note that earlier angle-resolved photoemission spectroscopy studies showed the existence of an extended saddle point in a broad range of cuprates⁴³ but this is near $(\pm\pi, 0)$ and $(0, \pm\pi)$, the very region where more recent ARPES studies show that the quasiparticles are heavily damped.⁴⁴ As the doping is increased the quasiparticle weight is pushed further out towards these $(\pm\pi, 0)$ and $(0, \pm\pi)$ regions where the state density is higher giving the very effect we observe, a growing peak in the DOS with doping. Such a picture then requires a pseudogap in the underdoped region and the vHs in the overdoped region. The reality however may be deeper, yet simpler. We note that the increasing pileup in spectral weight that occurs near E_F with increasing doping in the overdoped region is a continuation of what is observed in the underdoped region, and has been noted previously in $\text{La}_{2-x}\text{Sr}_x\text{CuO}_4$.¹⁹ It is difficult to avoid the conclusion that the superficially rather different behavior on the underdoped and overdoped sides, namely, a gapped or peaked DOS respectively, are nonetheless related. This is given substance by considering the plots of $T^{89}\text{K}(T)$ shown in Fig. 7. This quantity is proportional to $\chi_s T$ and as such represents the sum of spin states within the Fermi window $(E_F \pm 2k_B T)$.⁴⁵ The continual upward displacement of the curves with doping shows that the number of states within the Fermi window are smoothly incremented with hole doping. This is seen more clearly in the insert to Fig. 7 where we plot $T^{89}\text{K}(T)$ at 300 K against p . $T^{89}\text{K}(300\text{K})$ increases monotonically with p indicating that the number of states within the Fermi window monotonically increases with p .

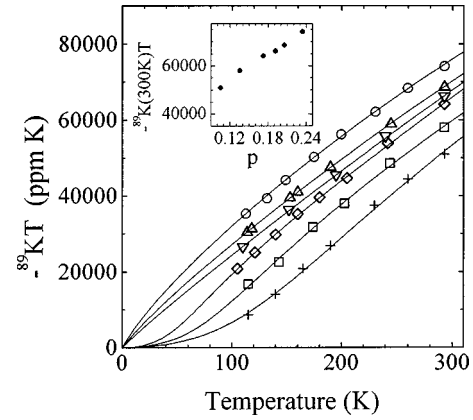


FIG. 7. Plot of $-^{89}\text{K}T$ against temperature for $\text{Y}_{0.8}\text{Ca}_{0.2}\text{Ba}_2\text{Cu}_3\text{O}_{7-\delta}$ with T_c and p values of 47.5 K, $p=0.234$ (O), 72.1 K, $p=0.206$ (Δ), 80.1 K, $p=0.192$ (∇), 86 K, $p=0.173$ (\diamond), 83.2 K, $p=0.136$ (\square), and 65.8 K, $p=0.105$ (+). The solid lines are fits to the data using the model described in the text. Insert: Plot of $-^{89}\text{K}(300\text{K})T$ against p .

The same conclusion was drawn by Loram *et al.*¹⁹ by considering the doping dependence of the electronic entropy $S(T)$. Thus across the entire doping range the number of states within the Fermi window are uniformly incremented with doping where spectral weight is progressively piled up near the Fermi level. With further doping out into the metallic states, data from $\text{La}_{2-x}\text{Sr}_x\text{CuO}_4$ indicates that this extra spectral weight eventually collapses away and a conventional metal is eventually recovered.¹⁹

CONCLUSION

In conclusion, the NMR data from overdoped $\text{Y}_{1-x}\text{Ca}_x\text{Ba}_2\text{Cu}_3\text{O}_{7-\delta}$ superconducting cuprates can be interpreted in terms of a growing peak in the density of states. The data cannot be modeled assuming phase separation, magnetic impurities or a growing density of local moments.

ACKNOWLEDGMENTS

We acknowledge funding support from the New Zealand FRST (G.V.M.W.), the Royal Society of New Zealand (J.L.T.), and the United Kingdom EPSRC (J.L.T., R.M., and R.D.).

¹J. W. Loram, K. A. Mirza, J. R. Cooper, and W. Y. Liang, *J. Supercond.* **7**, 243 (1994).

²G. V. M. Williams *et al.*, *Phys. Rev. Lett.* **78**, 721 (1997).

³J. M. Harris, Z.-X. Shen, P. W. White, D. S. Marshall, M. C. Schabel, J. N. Eckstein, and I. Bozovic, *Phys. Rev. B* **54**, 15 665 (1996).

⁴M. R. Presland, J. L. Tallon, R. G. Buckley, R. S. Liu, and N. E. Flower, *Physica C* **176**, 95 (1991).

⁵J. W. Loram, K. A. Mirza, J. M. Wade, J. R. Cooper, and W. Y. Liang, *Physica C* **235-240**, 134 (1994).

⁶J. W. Loram, K. A. Mirza, J. R. Cooper, and J. L. Tallon, *Physica C* **282-287**, 1405 (1997).

⁷J. L. Tallon, C. Bernhard, U. Binniger, A. Hofer, G. V. M. Williams, E. J. Ansaldo, J. I. Budnick, and Ch. Niedermayer, *Phys. Rev. Lett.* **74**, 1008 (1995).

⁸J. L. Tallon, G. V. M. Williams, C. Bernhard, D. M. Pooke, M. P. Staines, J. D. Johnson, and R. H. Meinhold, *Phys. Rev. B* **53**, R11 972 (1996).

⁹R. Dupree, A. Gencten, and D. McK. Paul, *Physica C* **193**, 81 (1992).

¹⁰S. D. Obertelli, J. R. Cooper, and J. L. Tallon, *Phys. Rev. B* **46**, 14 928 (1992).

¹¹A. G. Kontos, R. Dupree, and Z. P. Han, *Physica C* **247**, 1 (1995).

- ¹²F. Mila and T. M. Rice, *Physica C* **175**, 269 (1991).
- ¹³M. Takigawa, A. P. Reyes, P. C. Hammel, J. D. Thompson, R. H. Heffner, Z. Fisk, and K. C. Ott, *Phys. Rev. B* **43**, 247 (1991).
- ¹⁴G. A. Levin and K. F. Quader, *Physica C* **258**, 261 (1996).
- ¹⁵Y. Kubo, Y. Shimakawa, T. Manako, and H. Igarashi, *Phys. Rev. B* **43**, 7875 (1991).
- ¹⁶L. Le Noc, A. Trokiner, J. Schneck, A. M. Pougnet, D. Morin, H. Savary, A. Yakubovskii, K. N. Mykhalyov, and S. V. Verkhovskii, *Physica C* **235-240**, 1703 (1994).
- ¹⁷G.-Q. Zheng, T. Kuse, Y. Kitaoka, K. Ishida, S. Ohsugi, K. Asayama, and Y. Yamada, *Physica C* **208**, 339 (1993).
- ¹⁸T. Nakano, M. Oda, C. Manabe, N. Momono, Y. Miura, and M. Ido, *Phys. Rev. B* **49**, 16 000 (1994).
- ¹⁹J. W. Loram, K. A. Mirza, J. R. Cooper, N. Athanassopoulou, and W. Y. Liang, *Proceedings of the 10th Anniversary HTS Workshop on Physics Materials and Applications* (World Scientific, Singapore, 1996), p. 341.
- ²⁰G. V. M. Williams and J. L. Tallon (unpublished).
- ²¹M. Oda, J. Nakano, Y. Kamada, and M. Ido, *Physica C* **183**, 234 (1991).
- ²²V. Kresin and S. A. Wolf, *Phys. Rev. B* **51**, 1229 (1995).
- ²³G. V. M. Williams, J. L. Tallon, and R. Meinhold, *Phys. Rev. B* **52**, 7034 (1995).
- ²⁴G. V. M. Williams, J. L. Tallon, R. Dupree, and R. Michalak, *Phys. Rev. B* **54**, 9532 (1996).
- ²⁵A. V. Mahajan, H. Alloul, G. Collin, and J. F. Marucco, *Phys. Rev. Lett.* **72**, 3100 (1994).
- ²⁶R. E. Walstedt, R. F. Bell, L. F. Schneemeyer, J. V. Waszczak, W. W. Warren, Jr., R. Dupree, and A. Gencten, *Phys. Rev. B* **48**, 10 646 (1993).
- ²⁷R. S. Markiewicz, *J. Phys. Chem. Solids* **58**, 1179 (1997).
- ²⁸J. D. Jorgensen, P. Lightfoot, S. Pei, B. Dabrowski, D. R. Richards, and D. G. Hinks, in *Advances in Superconductivity III*, edited by K. Kajimura and H. Hayakawa (Springer-Verlag, Tokyo, 1991), p. 337.
- ²⁹P. G. Radaelli, D. G. Hinks, A. W. Mitchell, B. A. Hunter, J. L. Wagner, B. Dobrowski, K. G. Vandervoort, H. K. Viswanathan, and J. D. Jorgensen, *Phys. Rev. B* **49**, 4163 (1994).
- ³⁰A. J. Millis and H. Monien, *Phys. Rev. Lett.* **70**, 2810 (1993).
- ³¹H. Takagi, T. Ido, S. Ishibashi, M. Uota, S. Uchida, and Y. Tokura, *Phys. Rev. B* **40**, 2254 (1989).
- ³²A. J. Millis and H. Monien, *Phys. Rev. B* **50**, 16 606 (1994).
- ³³V. J. Emery and S. A. Kivelson, *Nature (London)* **374**, 434 (1995).
- ³⁴P. Monthoux and D. Pines, *Phys. Rev. B* **47**, 6069 (1993).
- ³⁵D. Pines, *Physica C* **282-287**, 273 (1997).
- ³⁶N. J. Curro, T. Imai, C. P. Slichter, and B. Dabrowski, *Phys. Rev. B* **56**, 877 (1997).
- ³⁷I. Eremin, M. Eremin, S. Varlamov, D. Brinkmann, M. Mali, and J. Roos, *Phys. Rev. B* **56**, 11 305 (1997).
- ³⁸G. V. M. Williams, J. L. Tallon, J. W. Quilty, H. J. Trodahl, and N. E. Flower, *Phys. Rev. Lett.* **80**, 377 (1998).
- ³⁹J. L. Tallon, J. W. Loram, and G. V. M. Williams (unpublished).
- ⁴⁰J. L. Tallon, G. V. M. Williams, N. E. Flower, and C. Bernhard, *Physica C* **282-287**, 236 (1997).
- ⁴¹A. G. Loeser *et al.*, *Science* **273**, 325 (1996).
- ⁴²J. W. Loram (private communication).
- ⁴³A. A. Abrikosov, J. C. Campuzano, and K. Gofron, *Physica C* **214**, 73 (1993).
- ⁴⁴D. S. Marshall, D. S. Dessau, A. G. Loeser, C.-H. Park, A. Y. Matsuura, J. N. Eckstein, I. Bozovic, P. Fournier, A. Kapitulnik, W. E. Spicer, and Z.-X. Shen, *Phys. Rev. Lett.* **76**, 4841 (1996).
- ⁴⁵J. W. Loram, K. A. Mirza, J. M. Wade, J. R. Cooper, N. Athanassopoulou, and W. Y. Liang, *Advances in Superconductivity VII* (Springer-Verlag, Tokyo, 1995), p. 75.